From Glass Formation to Icosahedral Ordering by Curving Three-Dimensional Space

Francesco Turci,[1,*] Gilles Tarjus,[2] and C. Patrick Royall[1,3,4,5]
[1]H.H. Wills Physics Laboratory, Tyndall Avenue, Bristol BS8 1TL, United Kingdom
[2]LPTMC, CNRS-UMR 7600, Université Pierre et Marie Curie, boîte 121, 4 Pl. Jussieu, 75252 Paris cedex 05, France
[3]School of Chemistry, University of Bristol, Cantock's Close, Bristol BS8 1TS, United Kingdom
[4]Centre for Nanoscience and Quantum Information, Tyndall Avenue, Bristol BS8 1FD, United Kingdom
[5]Department of Chemical Engineering, Kyoto University, Kyoto 615-8510, Japan
(Received 12 July 2016; revised manuscript received 15 December 2016; published 26 May 2017)

Geometric frustration describes the inability of a local molecular arrangement, such as icosahedra found in metallic glasses and in model atomic glass formers, to tile space. Local icosahedral order, however, is strongly frustrated in Euclidean space, which obscures any causal relationship with the observed dynamical slowdown. Here we relieve frustration in a model glass-forming liquid by curving three-dimensional space onto the surface of a 4-dimensional hypersphere. For sufficient curvature, frustration vanishes and the liquid "freezes" in a fully icosahedral structure via a sharp "transition." Frustration increases upon reducing the curvature, and the transition to the icosahedral state smoothens while glassy dynamics emerge. Decreasing the curvature leads to decoupling between dynamical and structural length scales and the decrease of kinetic fragility. This sheds light on the observed glass-forming behavior in Euclidean space.

DOI: 10.1103/PhysRevLett.118.215501

The very large increase in viscosity found in glass-forming liquids upon cooling or compression without significant change in structure remains a major outstanding challenge in condensed-matter physics. In particular, one seeks to clarify whether vitrification is linked to an underlying thermodynamic phase transition or whether the process is predominantly dynamical [1].

Among the most enduring pictures of dynamic arrest is that liquids form geometric motifs upon supercooling [2]. It is now possible to identify such motifs, e.g., icosahedra and other locally preferred structures (LPS), using computer simulation [3–6] and particle-resolved studies in colloid and granular experiments [7,8]. Further evidence of local icosahedral order is found in metallic glass formers [9–13]. While the idea of icosahedra (to focus on this specific LPS) as being the cause of dynamical slowdown in many materials has proven to be remarkably durable, it has, equally remarkably, seldom been seriously tested. This is the main motivation of the present work.

A strong piece of evidence for a structural or thermodynamic mechanism would be the identification of static length scales that grow significantly when approaching the glass transition. (It is indeed possible to demonstrate that the divergence of the relaxation time at a finite temperature implies a divergent static correlation length [14], but this relies on a bound that may not necessarily put stringent constraints in the dynamically accessible regime.) Any successful theory also needs to account for the well-established phenomenon of dynamical heterogeneities, in the form of "liquidlike" fast-moving and "solidlike" slow-moving regions whose lifetime and size increase upon supercooling [15,16], a phenomenon that has been characterized by "dynamical" length scales. Different types of static lengths have been considered in previous studies [4,17–20], and here we focus on the case of static lengths related to icosahedral order and their coupling or decoupling to dynamical length scales.

Fivefold symmetric motifs such as icosahedra do not tile 3D Euclidean space periodically [2]. For single-component systems of spheres, it has been theoretically shown [21,22] and observed in simulations [23] that 120 particles on the surface of a 4D hypersphere, the "3-sphere" S^3, of a specific curvature can realize a perfect tiling of space with every particle at the center of an icosahedron: the so-called $\{3, 3, 5\}$ polytope. Flattening space then induces frustration [22,24]. However, at the end of the flattening process, in Euclidean space, frustration is strong and the growth of icosahedral order is strongly suppressed [4,6]. In particular, for multicomponent mixtures of spheres at the degree of supercooling accessible to computer simulations (and colloid experiments), i.e., the first 4–5 decades of increase of the structural relaxation time τ_α relative to the normal liquid, rather limited domain sizes of icosahedral regions are found and the associated length scales remain small [3,6,25]. Furthermore, these structural lengths are significantly smaller than some dynamical lengths associated with the growingly heterogeneous character of the dynamics [4,25–27].

Despite the many claims and suggestions, this calls into question whether such structures can be the main cause of dynamic arrest. At the very least, it is fair to state that the description of the mechanism by which frustrated icosahedral order influences slow dynamics remains an unresolved problem. To make progress on this issue, we curve

3D space to relieve frustration and we use curvature as an additional control parameter to investigate equilibrium glass-forming liquids. While curved 3D space can only be realized by computer simulations, it is a unique means to probe the causal link between local icosahedral order and dynamics and to test the premise upon which geometric frustration is predicated—that of an underlying phase transition avoided due to frustration [28].

We consider a model glass-forming liquid, the Wahnström model, which is a Lennard-Jones binary mixture with size ratio $\sigma_A/\sigma_B = 6/5$. We choose this model because it is known to display a significant correlation between slow dynamics and the formation of local icosahedral motifs in Euclidean space [5,25,29].

We perform Monte Carlo (MC) simulations of $N \in [120, 720]$ particles on the 3-sphere S^3, with a modified Marsaglia method [30,31] to isotropically sample the surface of the 4D hypersphere. The results in curved space are complemented with molecular dynamics (MD) results in Euclidean space [32]. We fix the reduced density

$$\tilde{\rho} = \frac{N}{V(R)} \frac{V_{\mathrm{cap}}(R,\sigma_A) + V_{\mathrm{cap}}(R,\sigma_B)}{E(\sigma_A) + E(\sigma_B)} = 1.296\sigma_A^{-3}, \quad (1)$$

where N is the total number of particles, $V(R)$ the (hyper) area of the 3-sphere, $V_{\mathrm{cap}}(R,\sigma)$ is the (hyper)area of a spherical cap of height $h = R(1 - \cos\sigma/2R)$ and $E(\sigma)$ the Euclidean volume of a particle of diameter σ. At fixed density the number of particles N and the radius of curvature R are therefore coupled: the range $N = 120$–720 corresponds to $R \approx 1.666$–$3.037\sigma_A$. In the limit $R \to \infty$, one recovers the usual expression $\tilde{\rho} \to N/V$ (see the Supplemental Material for more details [34]).

We first investigate the effect of the curvature on the structure of the system. We take the first minimum of the pair correlation function as the bond length which, together with the Delaunay triangulation obtained from the convex hull of the particle coordinates, provides the network of nearest neighbors (see the Supplemental Material [34] for more details). This then allows for the detection of icosahedral order throughout the system via a modified topological cluster classification [38].

We find that for $N = 120$ the bidisperse Wahnström model abruptly freezes to an ordered icosahedral structure, the $\{3,3,5\}$ polytope [21], as the temperature T is lowered, just like a monodisperse system of spherical particles [22,23]. This is illustrated in Fig. 1 where we plot the concentration n of particles detected in icosahedral domains as a function of $1/T$ for various curvatures characterized by the total number of particles N. For $N = 120$ a sharp crossover, which is the finite-size version of a first-order transition, from an icosahedra-poor liquid to an icosahedral structure is found. Frustration is thus relieved by curvature and the concentration fluctuations due to the bidispersity have no significant influence at this curvature. (See the Supplemental Material [34] for a more detailed analysis of the low-T structure.)

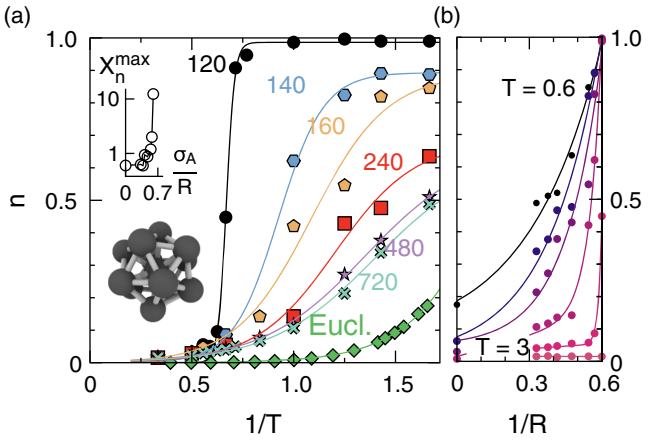

FIG. 1. (a) Concentration n of particles found in domains of icosahedra (see ball-and-stick model) as a function of the inverse of the reduced temperature T for several curvatures characterized by the system size N [see Eq. (1)]. The lines are hyperbolic-tangent fits, from which the maximum of the derivative $\chi_n = dn/dT$ can be estimated: see the case $N = 120$ in the inset. (b) Same data, as a function of the curvature $1/R$ at $T = 0.6$, 0.7, 0.8, 2, 3. Lines are guides to the eye.

As curvature decreases (and N and R increase), the crossover smoothens: the growth of icosahedral order becomes more gradual while the maximum concentration of icosahedra saturates at lower values, which is a sign of increasing frustration. The temperature range over which the change takes place broadens and shifts to lower temperatures. The Euclidean case is the end point of this continuous variation with curvature (see also the Supplemental Material [34]).

To describe the slowing down of the dynamics while avoiding the complexity brought by curvature and the parallel transport along geodesics we consider a simple time-dependent correlation function based on the number of neighbors that are lost with time:

$$C(t) = \left\langle \frac{1}{N} \sum_{i=1}^{N} \frac{\vec{v}_i(t_0 + t) \cdot \vec{v}_i(t_0)}{\vec{v}_i^2(t_0)} \right\rangle_{t_0}, \quad (2)$$

where $\vec{v}_i(t)$ is the indicator vector of length N identifying the nearest neighbors of particle i at time t. The function $C(t)$ corresponds to the average fraction of neighbors that has not changed between time t_0 and time t. While being independent of the local curvature of the space, it provides a measure of the relaxation. Through a stretched-exponential fit to $C(t) - C(\infty)$ (see the Supplemental Material [34]) we obtain an estimate of the structural relaxation time τ. In the case of the two larger curvatures, $N = 120$ and 140, the crossover is so sharp that the relaxation time jumps from a finite value to an exceedingly large one in the icosahedral state, which then behaves as a solid for our purposes. This is much like the dynamical behavior at a first-order transition, albeit here in a finite-size system: the relaxation time may not truly diverge but is too large to be accessible

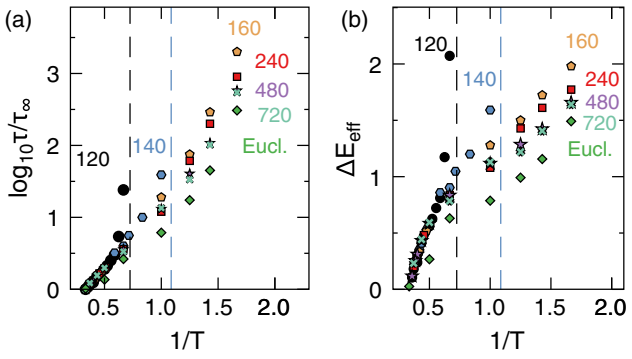

FIG. 2. (a) Logarithm of the relaxation time (a) and Effective activation energy $\Delta E_{\rm eff} = T \log \tau/\tau_\infty$ (b) versus $1/T$ for several curvatures. The vertical dashed lines approximately indicate the temperatures at which the $N = 120$ and $N = 140$ systems freeze into a solid icosahedral phase.

in a computer simulation. In contrast for $N = 160$, the crossover is smooth enough that we can access the relaxation time even when the growth of icosahedral order has saturated and we then see no sign of divergence.

The relaxation time is shown in Fig. 2(a). For $T \gtrsim 2$ curvature has little influence on the relaxation (see also the Supplemental Material [34]). But this is no longer true at lower temperature. While the two largest curvatures exhibit an abrupt freezing to a solid icosahedral phase, the transition appears to be *avoided* for weaker curvatures and a continuous increase of the relaxation time is found over the accessible range, as in the Euclidean space.

In order to assess the change with curvature of the kinetic fragility, i.e., the degree of super-Arrhenius temperature dependence of the relaxation time, we consider the effective activation energy $\Delta E_{\rm eff} = T \log(\tau/\tau_\infty)$, where τ_∞ is the relaxation time at high T [Fig. 2(b)]. The two curvatures where freezing takes place behave very differently from the others. For $N \geq 160$ to the Euclidean limit, $\Delta E_{\rm eff}$ is found to increase continuously with increasing $1/T$, which is the signature of a super-Arrhenius, fragile, behavior. The differences between the curvatures are not dramatic but there is a clear trend towards a monotonic decrease of fragility as curvature decreases. Since the high-T behavior is independent of curvature, this can be seen unambiguously and without data fitting by comparing the effective activation energies (or the relaxation times) at low T (see Fig. 2): The kinetic fragility decreases as the curvature decreases (and at the same time frustration increases, consistent with previous work [39,40]).

As mentioned above, the emergence of slow dynamics in glass-forming systems is often attributed to the growth of spatial correlations in the dynamics and the statics [20]. The former manifest themselves as dynamical heterogeneities [16]; the latter are found through investigations of point-to-set correlations [4,14,17–19] or through some characterization of the growth of the local order [6,20,41]. As also already emphasized, for most glass formers studied by simulations, including the Wahnström mixture, one finds a rapid increase for the dynamical lengths, but a modest increase of the static lengths [25,26]. One is limited by the dynamic range accessible to computer simulations, so that it is hard to attain the deeply supercooled regime near the glass transition. Thus, it is hard to clearly identify on the origin of the observed decoupling. We cannot improve the accessible range but we can add a new control parameter, the curvature.

In order to explore dynamic correlations, we focus on low-mobility (slow) particles, following Ref. [42]. To do so, we define a neighbor-dependent mobility and use a thresholded persistence function of the indicator neighbor vectors v_i in order to identify the slow particles. The number of slow particles is then defined as

$$N_{\rm slow}(t) = \left\langle \sum_{i=1}^{N} \Theta[\vec{v}_i(t_0 + t) \cdot \vec{v}_i(t_0) - \tilde{N}] \right\rangle_{t_0}, \quad (3)$$

where $\Theta(x)$ is the Heaviside function and $\tilde{N}$ the minimum number of neighbors of a particle that must not change for this particle to be taken as slow: we chose $\tilde{N} = 8$ but we checked that the results are not very sensitive to the choice of this particular threshold ($5 \leq \tilde{N} \leq 10$). We can then study the average of the number of slow particles during time t and the fluctuations, characterized by the susceptibility $\chi(t) = (1/N)[\langle N^2_{\rm slow}(t)\rangle - \langle N_{\rm slow}(t)\rangle^2]$.

To extract the dynamic length, we work in real space [43]: we compute the radial distribution function restricted to the particles that are slow at $t = \tau$, $g_{\rm slow}(r;\tau)$. From it we estimate a typical correlation length $\xi_{\rm slow}$ via an exponential fit, $g_{\rm slow}(r;\tau) \sim \exp[-r/\xi_{\rm slow}(\tau)]/r + c$, where c is a long-range normalization constant depending on the finite-size limitations of our systems: see Fig. 3(b) and the Supplemental Material [34]. The resulting length, after a rescaling by its high-temperature value, is shown in Fig. 3(a) for several curvatures. It grows as T decreases, which indicates increasing spatial correlations in the dynamics and bigger dynamical heterogeneities. The rate of change with T appears nonmonotonic with curvature, first decreasing with N down to $N = 240$ and then increasing up to the Euclidean limit. [We find a less marked but qualitatively similar behavior for the peak value $\chi^{\rm max}$ of the dynamic susceptibility $\chi(t)$, which occurs for $t \approx \tau$ as generically found in glass formers and can loosely be taken as a relative measure of the number of dynamically correlated particles; see the Supplemental Material [34].]

To obtain a structural length scale, we use a similar approach to that for the dynamic length, except that we consider only particles in icosahedra: we compute the corresponding restricted radial distribution function $g_{\rm icos}(r)$ and extract $\xi_{\rm icos}$ through an exponential fit [see Fig. 3(b) and the Supplemental Material [34]]. We find a steady reduction of both the extent and the rate (with decreasing temperature) of the growth of icosahedral correlations as curvature decreases and frustration increases, in line with the results shown in Fig. 1(a).

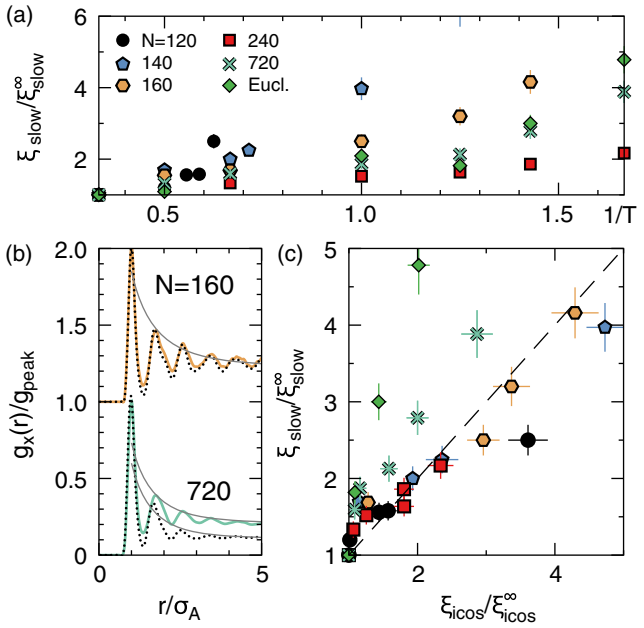

FIG. 3. (a) Rescaled dynamic length versus $1/T$ for different curvatures. (b) Radial distribution functions $g_{\mathrm{slow}}(r;\tau)$ (continuous) and $g_{\mathrm{icos}}(r)$ (dotted) for $N = 160, 720$ and $T = 0.8$ scaled by the first peak height and shifted for clarity. Fits to extract length scales (see Supplemental Material [34]) in gray. (c) Rescaled dynamic length versus the rescaled structural length for different curvatures, down to the Euclidean limit.

The dynamic and structural lengths are compared in Fig. 3(c), once rescaled to their high-temperature value. One observes a clear trend with increasing curvature (i.e., decreasing N): while a significant decoupling is found in Euclidean space, this decoupling decreases and appears to vanish for $N = 240$ and less. When the icosahedral order becomes less frustrated, dynamical and structural lengths increase hand in hand as the relaxation slows down. The growth of the local order then seems to fully determine the properties of the dynamics. On the other hand, as frustration increases, this one-to-one correspondence becomes blurred and other mechanisms, possibly related to the mean-field description of glass-forming liquids [45,46], must be considered in addition. Note that we do not expect the decoupling to be merely an effect of the finite size of the curved systems. It has indeed been shown (in Euclidean space) that in the range accessible to simulations the dynamics of 3D glass formers is not very sensitive to size effects [47,48], contrary to 2D systems [33,49].

To summarize, we have studied the structure and the dynamics of a supercooled liquid in curved 3D space, using curvature as a way to tune the degree of frustration of the local order. Through this additional control parameter one can assess the *causal* relationship between local order and glass formation. Evidence for some correlation between relaxation slowdown and growth of icosahedral order has been reported in the present Wahnström model [3,5,25], but it is hard to get an in-depth picture considering the limited range accessible to simulations and the strong frustration. Starting from the Euclidean limit and curving space, we find an increase of the extent and of the influence of the local icosahedral order on the liquid under cooling, until one encounters a low enough frustration that allows freezing into an ordered icosahedral structure and thereby prevents glass formation.

Interestingly, the increase of frustration with decreasing curvature is accompanied by the decoupling of the temperature evolution of the dynamical and structural lengths. This suggests that while the collective behavior of the system is controlled by the growth of the icosahedral order and the proximity to an underlying (avoided) ordering transition for sufficiently weak frustration, the slowing down is no longer uniquely dominated by the local order when frustration increases: the observed decoupling appears as a signal that other mechanisms come into play. The behavior found in the Euclidean space is the end point of this process with only remnants of the role of icosahedral ordering.

Based on Fig. 1, we speculate that at deep supercooling in Euclidean space, beyond the regime accessible here, the population of icosahedra would increase and ultimately plateau. This behavior may be accessible to advanced experimental techniques such as nanobeam electron diffraction [12,13]. Such a saturation might also herald a fragile-to-strong crossover in metallic glass formers known for their icosahedral order [50].

Finally, we contrast the situations in $d = 3$ and $d = 2$. The change of behavior with curvature observed in the present study is profoundly different from that found in 2D systems where sixfold local bond-orientational order is prevalent. In the latter case, the ordering transition in the absence of frustration (which means in the Euclidean plane) is continuous or weakly first order [51,52]. In three dimensions, the transition appears strongly first order: it is accordingly characterized not by the continuous divergence of the relaxation time or the correlation length but by (rounded) jumps from finite to exceedingly large values in these quantities. On the other hand, by curving 2D space [40,53,54] one then encounters an avoided continuous transition near which the correlation length can be very large. Here instead, by flattening 3D space, we see the effect of an avoided first-order transition, with a broadened crossover and limited correlation lengths. The collective static behavior generated by the proximity of an avoided transition is more prominent in two dimensions than in three dimensions. This may explain why the decoupling between dynamical and static lengths appears to be absent in many 2D liquids [39,53,55], and why finite-size effects are more dramatic in 2D than in 3D glass formers [33].

We are grateful to S. Taylor for stimulating conversations about algorithms in curved space, to J. Hicks for preliminary simulations, and to P. Charboneau for helpful

suggestions. C. P. R. acknowledges the Royal Society for funding and F. T. and C. P. R. acknowledge the European Research Council (ERC consolidator grant NANOPRS, Project No. 617266). C. P. R. acknowledges the University of Kyoto SPIRITS fund. This work was carried out using the computational facilities of the Advanced Computing Research Centre, University of Bristol.

*f.turci@bristol.ac.uk

[1] L. Berthier and G. Biroli, Rev. Mod. Phys. **83**, 587 (2011).
[2] F. C. Frank, Proc. R. Soc. A **215**, 43 (1952).
[3] D. Coslovich and G. Pastore, J. Chem. Phys. **127**, 124504 (2007).
[4] B. Charbonneau, P. Charbonneau, and G. Tarjus, Phys. Rev. Lett. **108**, 035701 (2012).
[5] G. M. Hocky, D. Coslovich, A. Ikeda, and D. R. Reichman, Phys. Rev. Lett. **113**, 157801 (2014).
[6] C. P. Royall and S. R. Williams, Phys. Rep. **560**, 1 (2015).
[7] C. Royall, S. Williams, T. Ohtsuka, and H. Tanaka, Nat. Mater. **7**, 556 (2008).
[8] M. Leocmach and H. Tanaka, Nat. Commun. **3**, 974 (2012).
[9] H. Sheng, W. Luo, F. Alamgir, J. Bai, and E. Ma, Nature (London) **439**, 419 (2006).
[10] Y. T. Shen, T. H. Kim, A. K. Gangopadhyay, and K. F. Kelton, Phys. Rev. Lett. **102**, 057801 (2009).
[11] Y. Q. Cheng and E. Ma, Prog. Mater. Sci. **56**, 379 (2011).
[12] A. C. Y. Liu, M. J. Neish, G. Stokol, G. A. Buckley, L. A. Smillie, M. D. de Jonge, R. T. Ott, M. J. Kramer, and L. Bourgeois, Phys. Rev. Lett. **110**, 205505 (2013).
[13] A. Hirata, L. J. Kang, T. Fujita, B. Klumov, K. Matsue, M. Kotani, A. R. Yavari, and M. W. Chen, Science **341**, 376 (2013).
[14] A. Montanari and G. Semerjian, J. Stat. Phys. **125**, 23 (2006).
[15] M. Ediger, Annu. Rev. Phys. Chem. **51**, 99 (2000).
[16] L. Berthier, G. Biroli, J. P. Bouchaud, L. Cipelletti, and W. Van Saarloos, *Dynamical Heterogeneities in Glasses, Colloids, and Granular Media* (Oxford Univ. Press, New York, 2011), Vol. 150.
[17] G. Biroli, J. P. Bouchaud, A. Cavagna, T. S. Grigera, and P. Verrochio, Nat. Phys. **4**, 771 (2008).
[18] L. Berthier and W. Kob, Phys. Rev. E **85**, 011102 (2012).
[19] G. M. Hocky, T. E. Markland, and D. R. Reichman, Phys. Rev. Lett. **108**, 225506 (2012).
[20] S. Karmakar, C. Dasgupta, and S. Sastry, Annu. Rev. Condens. Matter Phys. **5**, 255 (2014).
[21] H. S. M. Coxeter, *Regular Polytopes* (Dover Publications, New York, 1973).
[22] J.-F. Sadoc and R. Mosseri, *Geometrical Frustration* (Cambridge University Press, Cambridge, England, 2006).
[23] J. P. Straley, Phys. Rev. B **30**, 6592 (1984).
[24] D. R. Nelson, *Defects and Geometry in Condensed Matter Physics* (Cambridge University Press, Cambridge, England, 2002), p. 392.
[25] A. Malins, J. Eggers, C. P. Royall, S. R. Williams, and H. Tanaka, J. Chem. Phys. **138**, 12A535 (2013).
[26] P. Charbonneau and G. Tarjus, Phys. Rev. E **87**, 042305 (2013).
[27] B. Charbonneau, P. Charbonneau, and G. Tarjus, J. Chem. Phys. **138**, 12A515 (2013).
[28] G. Tarjus, S. A. Kivelson, Z. Nussinov, and P. Viot, J. Phys. Condens. Matter **17**, R1143 (2005).
[29] U. R. Pedersen, T. B. Schroder, J. C. Dyre, and P. Harrowell, Phys. Rev. Lett. **104**, 105701 (2010).
[30] G. Marsaglia, Ann. Math. Stat. **43**, 645 (1972).
[31] K. W. Kratky and W. Schreiner, J. Comput. Phys. **47**, 313 (1982).
[32] MC calculations and MD in 3D Euclidean space have proven to be comparable at long times [33].
[33] E. Flenner and G. Szamel, Nat. Commun. **6**, 7392 (2015).
[34] See Supplemental Material at http://link.aps.org/supplemental/10.1103/PhysRevLett.118.215501 for more details on Monte Carlo calculations, dynamic correlations, defects and length determination, which includes Refs. [35–37].
[35] M. A. Peterson, Am. J. Phys. **47**, 1031 (1979).
[36] K. Sugihara, J. Geom. Graphics **6**, 69 (2002).
[37] J.-P. Hansen and I. Macdonald, *Theory of Simple Liquids* (Academic, London, 1976).
[38] A. Malins, S. R. Williams, J. Eggers, and C. P. Royall, J. Chem. Phys. **139**, 234506 (2013).
[39] T. Kawasaki, T. Araki, and H. Tanaka, Phys. Rev. Lett. **99**, 215701 (2007).
[40] F. Sausset, G. Tarjus, and P. Viot, Phys. Rev. Lett. **101**, 155701 (2008).
[41] E. D. Cubuk, S. S. Schoenholz, J. M. Rieser, B. D. Malone, J. Rottler, D. J. Durian, E. Kaxiras, and A. J. Liu, Phys. Rev. Lett. **114**, 108001 (2015).
[42] E. Flenner, M. Zhang, and G. Szamel, Phys. Rev. E **83**, 051501 (2011).
[43] Small system sizes limit the conventional reciprocal space approach [44].
[44] N. Lačević, F. W. Starr, T. B. Schroder, and S. C. Glotzer, J. Chem. Phys. **119**, 7372 (2003).
[45] T. R. Kirkpatrick, D. Thirumalai, and P. G. Wolynes, Phys. Rev. A **40**, 1045 (1989).
[46] P. Charbonneau, J. Kurchan, G. Parisi, P. Urbani, and F. Zamponi, Annu. Rev. Condens. Matter Phys. **8**, 265 (2017).
[47] S. Karmakar, C. Dasgupta, and S. Sastry, Proc. Natl. Acad. Sci. U.S.A. **106**, 3675 (2009).
[48] L. Berthier, G. Biroli, D. Coslovich, W. Kob, and C. Toninelli, Phys. Rev. E **86**, 031502 (2012).
[49] S. Vivek, C. P. Kelleher, P. M. Chaikin, and E. R. Weeks, arXiv:1604.07338.
[50] C. Zhou, L. Hu, Q. Sun, H. Zheng, C. Zhang, and Y. Yue, J. Chem. Phys. **142**, 064508 (2015).
[51] D. R. Nelson and B. I. Halperin, Phys. Rev. B **19**, 2457 (1979).
[52] E. P. Bernard and W. Krauth, Phys. Rev. Lett. **107**, 155704 (2011).
[53] F. Sausset and G. Tarjus, Phys. Rev. Lett. **104**, 065701 (2010).
[54] J.-P. Vest, G. Tarjus, and P. Viot, Mol. Phys. **112**, 1330 (2014).
[55] H. Tanaka, T. Kawasaki, H. Shintani, and K. Watanabe, Nat. Mater. **9**, 324 (2010).